5-2017

Optimization of the NEDM Experiment

Patrick Rogers
University of Tennessee, Knoxville, proger10@vols.utk.edu

To the Graduate Council:

I am submitting herewith a thesis written by Patrick Rogers entitled "Optimization of the NEDM Experiment." I have examined the final electronic copy of this thesis for form and content and recommend that it be accepted in partial fulfillment of the requirements for the degree of Master of Science, with a major in Physics.

Geoffrey Greene, Major Professor

We have read this thesis and recommend its acceptance:

Nadia Fomin, Soren Sorensen, Yuri Efrimenko

Accepted for the Council:
Dixie L. Thompson

Vice Provost and Dean of the Graduate School

(Original signatures are on file with official student records.)

Optimization of the NEDM Experiment

A Thesis Presented for the
Master of Science
Degree
The University of Tennessee, Knoxville

Patrick Rogers
May 2017

ACKNOWLEDGEMENTS

Thank you to Vince Cianciolo and the other members of the JINS at ORNL for their help with this project.

ABSTRACT

The Neutron Electric Dipole Moment (NEDM) experiment is an upcoming experiment at ORNL to measure the size of an electric dipole moment inside of the neutron. This is being done to probe CP asymmetries that could give rise to a matter dominated universe. The experiment will utilize a nuclear reaction that outputs scintillation light in a manner that depends on the alignment of the spins of the reactant particles. This light will be detected and used to measure the NEDM. The amount of light collected for measurement will impact the accuracy of the results; the more photons collected the better the accuracy. However, during the process of transporting light from the reaction site to the light detectors, much of the scintillation light will be lost. Herein are the results of tests conducted on various parts of the NEDM apparatus in order to characterize and optimize light collection for the coming experiment.

TABLE OF CONTENTS

LIST OF FIGURES

CHAPTER ONE
THEORY AND MOTIVATION

Introduction

The Neutron Electric Dipole Moment (nEDM) experiment at Oak Ridge National Laboratory's Spallation Neutron Source aims to measure the size of an electric dipole moment within the neutron. The Standard Model predicts an incredibly small nEDM (~10^-31 ecm) [1]. Alternative theories predict values of much higher orders of magnitude such that if any nEDM were detected it would be taken as a signal of physics beyond the Standard Model. Previous attempts have been made to measure the size of the nEDM in various experiments [1]. Each experiment has lowered the upper bound for what the size of the nEDM could be, inching closer toward the Standard Model value. The nEDM experiment at Oak Ridge will attempt to measure a neutron's electric dipole moment of a larger size than the Standard Model prediction using a small amount of scintillation light from a nuclear reaction. To make measurement possible, the light collection efficiency needed to be maximized. This optimization was the goal of this thesis.

Matter Anti-Matter Asymmetry

According to the Standard Model of particle physics, the four fundamental forces would have created equal parts matter and anti-matter in the beginning of our universe. From the abundance of light elements from Big Bang Nucleosynthesis, and from the Cosmic Microwave Background, it has been ascertained that there is a baryon to photon ratio of roughly 6*10^-10 [2]. This means that for every billion or so parts anti-matter generated right after the Big Bang, there was a billion and one parts matter. The matter and anti-matter collided and annihilated releasing photons. Because there was just a little bit more matter than anti-matter, the universe became matter dominated instead of being full of nothing but photons. This matter/anti-matter asymmetry requires a larger Charge Parity (CP) violation than allowed by the Standard Model. Alternative models exist which provide enough CP violation to allow for the matter observed today, and a consequence of many of these theories is a small, but measureable neutron electric dipole moment [1]. If the nEDM were measured to be a value higher than the Standard Model prediction, it would allow probing of physics beyond the Standard Model which would hopefully help answer some of the mysteries left unanswered by it.

Neutron Electric Dipoles and CP symmetry

The connection between the neutron electric dipole moment and the matter/anti-matter asymmetry of the universe is due to the fact that a non-zero EDM (a positive and negative charge separated by some distance) would violate CP symmetry. In basic terms, CP symmetry means that if one has a system of charges and reverses the charge sign (Charge conjugation) and spatial coordinates (Parity) of the particles in the system, the energy of that system should remained unchanged. The energy of a dipole in an external electric field is given by:

$$U = -\vec{d} \cdot \vec{E} \quad [3]$$

Under a CP transformation, the electric field is even while the EDM transformation is odd. In other words, under such a transformation the sign of the field remains while the sign of the EDM reverses. Since the energy is the dot product of the two, energy is not conserved under the transformation.

Measurement Mechanics

EDMs are typically measured via precession frequency. When a neutron is placed in an external magnetic (B) and electric (E) field, the spin will precess. The energy of the neutron as it precesses is given by the equation:

$$h\nu = 2\mu_n B \pm 2d_n E \quad [1]$$

Where h is Planck's constant, ν is the precession frequency, μ_n is the magnetic moment of the neutron, and d_n is the nEDM. If B is held constant, then one can see that any change in the frequency implies d_n does not equal zero. So, if the external E field were flipped to point in the opposite direction, the change in energy of the system would be:

$$h\Delta\nu = (2\mu_n B + 2d_n E) - (2\mu_n B - 2d_n E) = 4d_n E$$

Thus, one can measure the size of the nEDM by measuring the change in the precession frequency when an external B field is held constant while the E field is flipped:

$$d_n = \frac{h\Delta\nu}{4E}$$

The Nuclear Reaction & Measurement

The preceding equation gives a way to measure the size of the nEDM using the precession frequency, but a way of 'seeing' this frequency is needed. This is done by utilizing a nuclear reaction that produces light in a matter related to the spin of the neutron. For this, the following reaction is utilized:

$$^{3}He + n => p + \ ^{3}H \quad +764 \text{ keV}[1]$$

The proton and triton that are generated from the reaction share the kinetic energy output, and will eventually lose energy by ionizing surrounding helium-4 which will release photons. These photons can be detected and are the way the nEDM will be measured.

The above nuclear reaction is spin-dependent. That is to say, that the probability of the above reaction occurring between a neutron and Helium-3 particle will depend on the orientation of the spins of the two reactant particles. When they are anti- aligned, the reaction has a high chance of occurring. When they are aligned the chance is very low [1]. Without the nEDM present, the spins would already precess at different rates due to the external magnetic field and the different gyromagnetic ratios of the particles.

If one were to graph the reaction rate over time in this scenario, one would see a pattern of the light output rate growing and shrinking periodically at the beat frequency (the difference between the two frequencies)

$$F_{Beat} = \ |f_2 - f_1| \quad [12]$$

However, if the nEDM is non-zero, then if the E field were changed, the neutron's precession changes as well. Rather than attempting to measure one cell with an alternating E-field, this effect will be seen by measuring 2 different measurement cells with oppositely oriented electric fields but the same magnetic field. The difference in the precession frequencies between the two cases will yield different beat frequencies which can be used to quantify the nEDM.

Motivation for Optimization

As mentioned before, it was desirable to optimize the experiment to assure accurate measurements. The experiment depends on the detection of scintillation light from a nuclear reaction, but the reaction site and detectors are not in the same location. This is due to the fact that they needed to be kept under different environmental conditions, so they were isolated from each other in two different environments within the experimental apparatus. This means light must be transported from the reaction site to light sensors across a boundary. Furthermore, the scintillation light is in the UV spectrum, whereas the detectors for the apparatus are efficient in the visible spectrum. This means light must be both wavelength shifted and transported away from the cell. During every step of shifting and transporting, a large portion of the light is lost (less than 1% reaches the detector), and since each scintillation flash is only expected to yield around a few thousand photons [9], that means not many are expected to reach the detectors. There will also be a fair amount of noise along with the signal, mostly from other reactions taking place in the cell including neutron β-decays and activation which releases gamma rays. Distinguishing between signal and noise events is crucial to improving the frequency measurement. The signal is mono-energetic due to the detector’s mechanism, so it can be distinguished from the other events (such as those produced by background/outside radiation). The more scintillation light one gets to the detector, the narrower the reaction’s peak is, and the easier it will be to distinguish from the noise. Therefore, the aim of this thesis is to explore different avenues for optimizing the light collection efficiency.

CHAPTER TWO
EXPERIMENTAL SET-UP

Apparatus Overview

Figure 1 depicts the experimental apparatus. The apparatus consists of a few key sub-systems: the measurement cell, the optical transport system, and the readout electronics. The measurement cell is located in the lowest chamber of the apparatus and is immersed in liquid helium-4. This is where the scintillation reaction will occur. The optical transport system consists of an array of green wavelength shifting fibers, acrylic windows, and clear optical fibers. They will carry light from the reaction site through a boundary separating the lower, helium-filled chamber from the upper chamber (which is in a vacuum), and then to the electronics. There are a series of pipes that feed the electronic cables and gas pumps near the top of the apparatus. These pipes pass through or around a series of radiation baffles that are meant to keep radiation from reaching the lower chamber as it may excite the liquid helium enough to boil. If the helium boils it will reduce the amount of time it an experiment can run.

Measurement Cell

Figure 2 depicts the measurement cell. The measurement cell consists of an acrylic cylinder with liquid helium inside that contains the alpha source. This will act as a proxy for the way that neutrons and Helium-3 react as it will ionize the liquid helium in a similar fashion. The ionized liquid helium will then emit UV photons (~280 nm). Normally, acrylic is not very a very good transmitter for UV light (a 2mm thick piece of

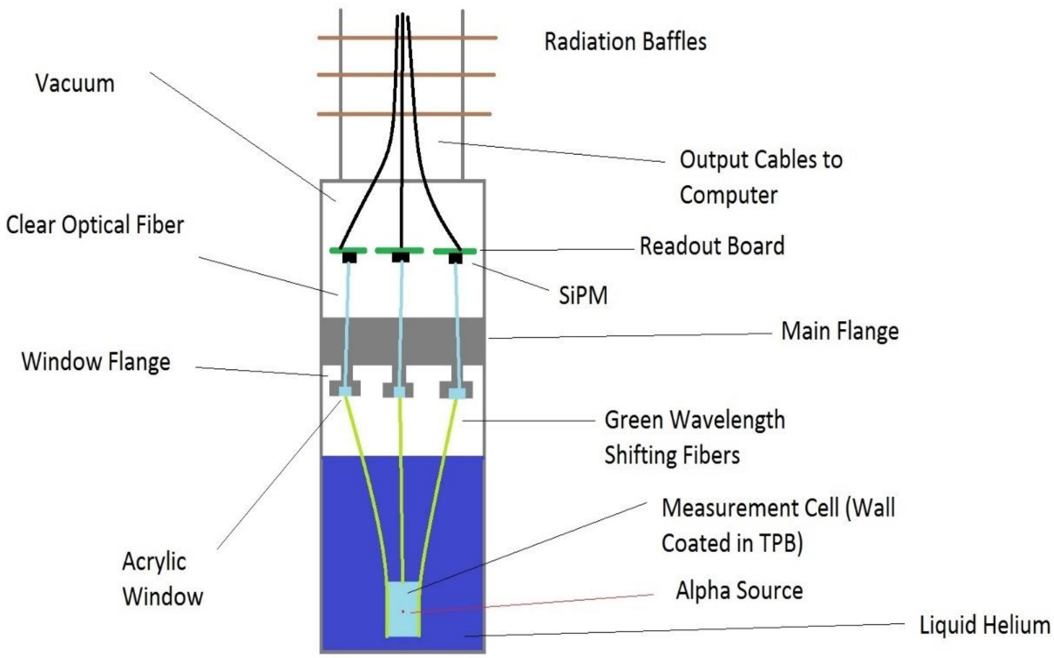

Figure 1: Simplified overview of the experimental setup. A nuclear reaction produces light in the measurement cell which is shifted in wavelength and carried up the optical fiber systems to a readout SiPM (Silicon Photomultiplier) detectors and electronic boards.

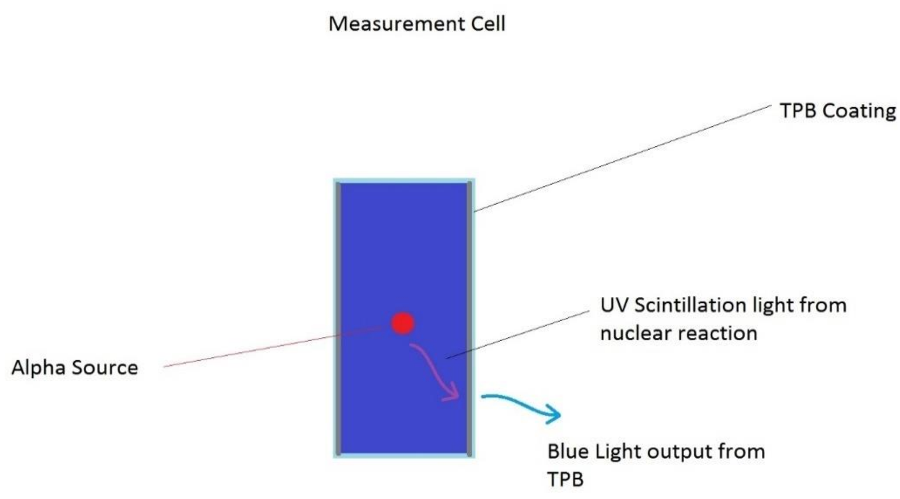

Figure 2: The measurement cell, consisting of a PMMA (acrylic) cylinder full of liquid helium with an alpha source inside. The walls are lined with TPB to convert UV light to visible blue light.

Acrylic will almost completely block UV while allowing visible light through) [4]. However, the walls of the cell are coated in a substance known as Tetraphenyl-butadiene or TPB. This substance absorbs light over a wide range of wavelengths, mostly in the UV range. When this happens the TPB molecules excite, and when they de-excite, they give off photons in the visible light range, mostly around 425nm [5]. TPB can be coated onto a surface via many means. Commonly it is dissolved into toluene, which is then layered onto a surface. The toluene will evaporate leaving behind a layer of TPB. Other methods involve dissolving Polypropylene or Polystyrene into the toluene along with the TPB. When the toluene dissolves it will leave behind a thin plastic film containing the TPB [6].

Optical Transport System

The optical transport system consists of 3 major components: Green wavelength shifting optical fibers, acrylic windows, and clear optical fibers. The outer walls of the measurement cell are lined with one end of an array of green fibers. These fibers, as their name suggests, shift the wavelength of light coming from the cell. This is done to retain light in the fibers. The green fibers will be attached to the measurement cell parallel to the long axis. Light from the reaction will have to enter the fibers from the side. Normally, with standard optical fibers this would not be possible. Due to simple refraction, light entering a standard optical fiber from the side won't be captured, it will pass through. In order to capture light then, a standard fiber must allow light to enter through one of its ends, then it will retain it with total internal reflection. Because of this, if standard fibers had been used instead of the wavelength shifting fibers, many times more fibers would've been needed to cover the same surface area of the measurement cell because of the need to point their ends towards the light source (the long axis of the fibers would've been perpendicular to the long axis of the cell, rather than parallel). The wavelength shifting fibers, however, have molecules that absorb the incoming light and re-emit green light isotropically. This means they can take in light from their sides, and much of the re-emitted light will reach the critical angle needed to reflect light inside the fiber, as seen in figure 3 & 4. In addition, they will transport light away from the cell toward the next piece in the system, the acrylic windows.

The acrylic windows are located on flanges that hang below a main flange that separates 2 large compartments. The windows serve as an interface between the green and clear fibers to allow light transfer between the two sets of fibers. However, the windows are located at the dividing line between two compartments: a lower compartment which contains the measurement cell, and the upper one which contains electronics, including the detectors. This lower compartment is filled with liquid helium to keep the reactants very cold (~4K). The nEDM experiment requires a gas-tight seal at the boundary (main flange) between the two compartments, yet a way to feed light from the lower compartment to the upper one is also needed. As such, the main flange has 4 stainless steel window openings that house the acrylic pieces. Sandwiched in between the steel window holder and the acrylic window is a compressible, hand-cut gasket ring made of a Teflon based material. In order to maintain a seal, a steel ring is used to squeeze the acrylic piece and gasket down onto the inner surface of the flange by bolting it down, keeping it under tension. However, different materials

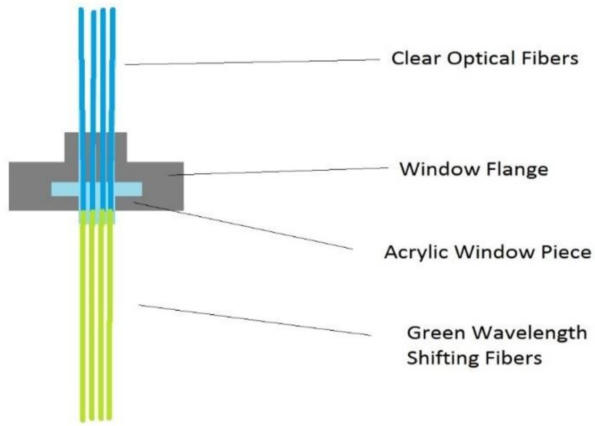

Figure 3: One of the four optical transport systems, consisting of an array of green optical fibers that shift the light coming from the cell from blue to green, a window that acts as an interface for 2 fiber systems, and an array of clear fibers that carry the now green light to the detectors. The flange is at the boundary between separate environments.

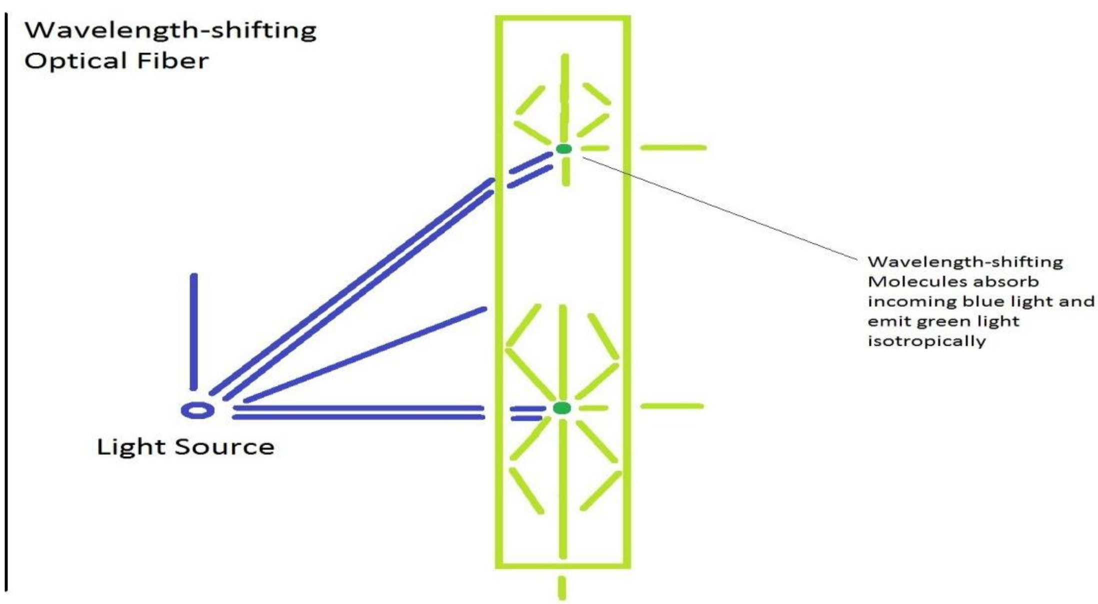

Figure 4: This shows the wavelength shifting fibers. They hold onto more light by using molecules that absorb incoming light and re-emit light at a different wavelength in all directions inside the fiber.

will expand and contract at different rates under a change in temperature, as seen in the following equation:

$$\frac{\Delta L}{L_0} = \alpha \Delta T \quad [7]$$

Where L is the length along a given dimension, T is the temperature, and α is the linear coefficient of thermal expansion, which varies with material. The linear coefficient of thermal expansion for acrylic is $75 \times \frac{10^{-6} m}{m * K}$ while that of stainless steel is around $15 \times \frac{10^{-6} m}{m * K}$ [8]. Essentially, for every degree Kelvin change in temperature, the acrylic shrinks 75 parts per million along a given spatial dimension while the steel shrinks at a fifth that rate. This will cause tension to be lost on the gasket, and since the gas being sealed against is helium, it doesn't take a lot of shrinkage to let it leak through. This means a way to keep tension under cryogenic conditions needed to be devised to maintain a seal as much as possible.

The final piece of the optical transport system is a set of four arrays of clear optical fibers, each array consisting of 16 evenly spaced fibers arranged in a 4x4 square pattern. The reason for doing this is to mimic the geometry of the light detectors which are arranged as 4x4 grids. There is a thin line of separation between each grid section on the SiPM which is a dead zone that doesn't detect light, so it was necessary to keep the fibers from directing light into one of these dead regions. The clear fibers are meant to simply transport green light from the window with the wavelength shifting fibers to the detectors attached to the electronics in the upper compartment. However, care must be paid to their transmission length. If the fibers become too long, they will begin to attenuate light. The equation for this goes as:

$$I = I_o e^{-\frac{x}{L}} \quad [9]$$

Where I is the amount of light that reaches the detector, x is the fiber length, and L is the transmission length.

SIPMs

The detectors are silicon photomultipliers (SIPMs). This particular type of detector was chosen due to numerous advantages it had over traditional Photomultiplier tubes (PMTs) and similar Avalanche Photodiodes (APD's). SIPMs differ from traditional PMTs via a process called an avalanche, which is also used in APD's. Rather than using dynodes to multiply a signal, SIPMs and APD's amplify a signal by applying a voltage to the core material which accelerates electron-hole pairs through it, which in turn causes collisions that form more electron-hole pairs which are also accelerated. SIPMs typically achieve a higher Quantum efficiency (# initial charge carriers produced vs # incident photons) than PMTs, but lower efficiencies than APD's. SIPMs can achieve high gains such that even the signal from a single photoelectron can be amplified to large levels, on par with PMTs and better than APD's [9]. This system is also virtually insensitive to external magnetic fields (and interference from Helium). SIPMs also take up a much smaller volume of space than traditional PMTs and operate at much lower bias voltages (tens of volts as opposed to thousands). They have a lower and linear temperature sensitivity making their behavior predictable. The main drawback to the SIPMs is the noise introduced by thermal effects, but there are ways to reduce this using temperature control schemes [10]. This is very useful for the nEDM experiment for the aforementioned reasons; there will be B fields present to precess the reactants, there is limited space for the components, the amount of light measured will be relatively small so a high efficiency would make best use of it, and Helium interference won't be a problem.

The SiPM works through a process called Geiger-mode. When the voltage applied to the detector is high enough, it will generate a strong electric field inside the silicon that can accelerate charges inside the SiPM. When a photon of light is absorbed, it will generate an electron-hole pair in the silicon. The field will accelerate the electron and hole in opposite directions. Because of how strong the field is, the electron and hole will accelerate enough that when they collide with other particles they can generate more pairs via impact ionization, and this process can self-perpetuate in what's called an avalanche. The silicon will break down and allow a sizable current flow. In order to stop the flow and reset the sensor for another measurement, quenching resistors are added that can lower the voltage back down to below breakdown [10].

As described above, the SiPM would only function as a binary detector; it would any have two outputs, 'on' and 'off'. In order to overcome this, the SiPM actually uses an array of very small photodiodes (typically there are 100-1000 cells per mm^2) [10], each of which operates in the same way as described previously. The outputs of each of these individual cells is summed to get a total output that is proportional to the number of cells that were triggered. In this way, one can quantify the amount of incident light based on the number of cells activated and thus, the size of the signal.

The main source of noise in the SIPMs will be what's called Dark Rate. This means that even when the device is completely dark (not exposed to any light) it will produce signals identical to those produced by photoelectrons. This is due to thermal effects;

essentially with enough thermal energy, electrons can boil off and form signals [9]. The higher the temperature, the more likely this is to happen. Signals from dark rate usually take on the form of single photon events, so setting thresholds above this can reduce false triggers, but the dark rate will still contribute to measured signals as well [10]. In the case of the nEDM experiment, the measurements taken will be single photoelectron events, so using a high threshold won't be possible. Instead, keeping the temperature inside the apparatus low will be used to prevent electrons from boiling off, essentially killing the dark rate.

The SiPM is typically run at a bias voltage a little over the breakdown voltage. This is done to make sure fluctuations in the voltage don't affect the Dark Count Rate too drastically. If it were run at breakdown, then a slight drop in voltage could see a large drop in the dark rate, and a slight increase would lead to a drastic increase in dark rate. At a voltage of about 2 volts over the breakdown, a slight increase or decrease in the voltage will have a smaller effect on the dark rate [10]. For the purposes of the experiment, the Overvoltage will actually be set even higher to 5-6 above breakdown to have good efficiency and high gain while still keeping the efficiency constant with respect to voltage.

Each cell in the SiPM generates a uniform and quantized amount of charge with each breakdown. As such the gain on the SiPM is very easy to predict, it tends to just be the ratio of charge output to the charge on an individual electron. The output charge just equals the overvoltage (difference in breakdown voltage and bias voltage) multiplied by the capacitance of a cell in the SiPM. This allows for narrow peaks for each photoelectron [10].

Temperature will play an important role in the operation of the SIPMs. Temperature makes two contributions: changes in the breakdown voltage and the dark rate. The breakdown voltage is roughly linear with temperature, causing a drop of roughly 1-1.5 volts for every 50C drop in temperature. Since the gain depends on the overvoltage (and the size of the signals depends on gain), it is important to keep the difference between the bias and breakdown voltage constant. One option to keep a constant overvoltage would be to monitor and adjust the bias voltage as the temperature changes. The other, easier way would be to use a temperature control system to keep the SIPMs at a stable temperature and leave the bias voltage constant. Also since the dark rate depends on temperature, keeping the temperature of the SIPMs constant would allow for an easily predictable dark rate that can then be accounted for in analysis, and keeping the temperature low will also keep the dark rate low if not eliminating it [10].

An important aspect of light detectors, including both PMTs and SIPMs, is knowing how to calculate the number of initial photoelectrons produced for a given signal. For this the following equations are used:

$$(\frac{\sigma_N}{N})^2 = \frac{J}{n_o} \quad [9]$$

$$J = 1+(\frac{\sigma_A}{A})^2 \quad [9]$$

J is what is called the *excess noise factor* and when the sizes of the avalanches produced by a detector are the same (and is this case they are since are signals produced by the SiPM cells are highly uniform and quantized) then this value is equal to one. N is the average signal size; sigma is the standard deviation or rms of the signal.

n_0 is the number of primordial charge carriers or photoelectrons produced by the detector. Using these equations, the number of photoelectrons produced by light detectors in later discussed tests was calculated since this equation works for conventional PMTs like those used in the testing [9].

Boards

There are four boards, one for each SIPM, that are shaped like a quarter of a ring. They are arranged to form a full ring and suspended above the flange that separates the lower and upper compartments. They take the signals from the SIPMs and process them into data. They will only read signals over a certain size threshold, to try to cut down on the amount of noise recorded. Setting the threshold to a high enough level to discriminate noise, while low enough to record light signals, was necessary. Their performance can also be altered under cryogenic conditions; it is for this reason that the board covers they are attached to are lined with copper foil with a heating resistor attached. These resistors are used to raise the board temperatures so that they don't become so cold that their performance suffers. A picture of the boards can be found in Figure 5.

Figure 5: The electronic boards arranged above the main flange. The SiPM detectors plug in on the other side.

CHAPTER THREE
OPTIMIZATION EXPERIMENTS

Measurement Cell

To optimize the measurement cell, a series of tests was run on the TPB coatings to measure their UV conversion efficiency and ascertain how durable they would be against exposure to the elements and to UV light. The way this was tested was by setting up an apparatus in a large, black box (called the “Dark Box”), as illustrated in Figure 6.

The purpose of the box was to act as an enclosure to keep out as much outside light as possible. The box was open on the top to allow access to the inside, but had a lid with a gasket that could be secured in place during experiment runs to prevent light from getting in through the top. The box had openings on the side for wires to go in and out of the box such. An LED in the UV and Violet wavelength range was connected to a pulser which controlled how fast and how bright the LED would flash. A PMT connected to a high-voltage supply was used to collect the light and send signals to a computer for analysis.

At first the space between the LED and PMT was left empty, and light from the LED was collected by the PMT and the signals collected were analyzed. After that, various samples of acrylic disks, some containing a layer of TPB and other materials, were inserted between the LED and PMT. When the UV light from the LED struck the TPB coated disks, the light would be converted to blue light which would pass through the acrylic to the PMT.

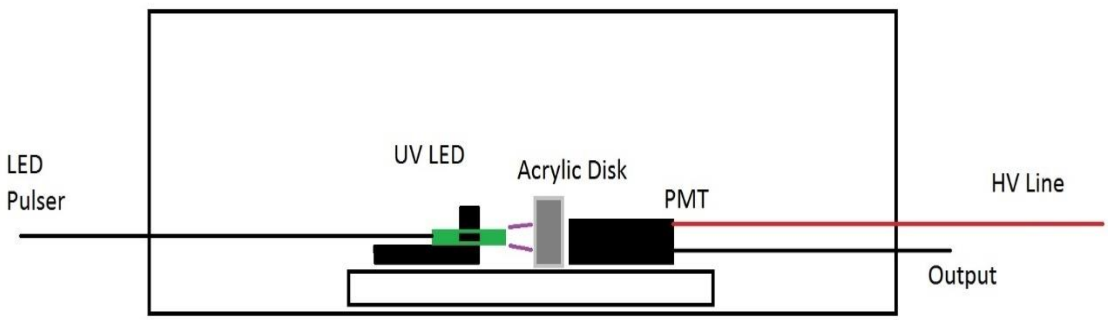

Figure 6: The experimental set-up for testing the TPB coatings on some sample disks representing the walls of the measurement cell. Pulsed light from the LED will strike the acrylic sample (or empty space) and will either be converted and allowed to reach the PMT, allowed to reach the PMT directly, or blocked from reaching the PMT.

The first step toward testing the reliability of the TPB coatings was to check measurement repeatability by doing a few runs back-to-back with the same sample to see if multiple runs produced similar results. The apparatus was set up, minus the acrylic disk, the box was closed, and the LED and PMT were turned on. Some signals were recorded from the PMT to be analyzed, after which the devices were deactivated and the box re-opened. This was repeated a few times. After a few signals were recorded with no sample inserted, one of the sample disks was removed from its packaging and inserted between the LED and PMT. This was an acrylic disk with a Polypropylene and TPB film coated onto one side of the disk. This side was faced toward the LED. The box was closed, and the LED and PMT were activated, and pulsed signals were recorded for a time. Once again, the devices were deactivated, and the disk was removed, then replaced for another run, and the process was repeated a few times. Afterwards, the sample was returned to part of its packaging. After that the process was done for a disk with a Polystyrene TPB layer, as well as a blank disk with no coating.

After a few repeated runs, it was decided to see if leaving the samples exposed to room temperature and humidity would adversely affect their performance. This was to determine how much care would be needed with the TPB coated measurement cells to assure good performance during the nEDM experiment. The cells were left out of their packaging in the dark box over night to expose them to room temperature and humidity, but not light. After overnight exposure, the samples were once again measured in the same fashion as stated above to check repeatability.

The final step was to expose the samples to light. This was done in two stages. For the first stage the samples were left out in the lab environment, exposed to the overhead lights for 4 hours at a time. This was done twice for a total exposure time of 8 hours. After this was done, the samples were taken outside and exposed to sunlight for 10 minute increments and measured with each increment.

All of the aforementioned methods of testing the TPB samples was run two different times with two different sets of samples. The first set also contained a thin microscope slide with pure TPB layered on the surface. The results all of the tests discussed herein will be shown and discussed in the next chapter.

Optical System

There were concerns over a few aspects of the optical system. The first dealt with the fibers, specifically, with the lengths of the clear fibers, as well as the interface between the two fibers. To test these two things, the set up in figures 7 & 8 was used. In summary, a blue LED was inserted into an acrylic block to hold it in place. A green optical fiber was clad in un-shrunken shrink wrap to keep external light from entering the fiber anywhere but at the ends. One end was dipped in optical grease and inserted into the same acrylic block as the LED, and butted against the LED. The other end of the green fiber was greased and inserted into a black 3D printed cylinder that had 2 openings (one was 1mm in diameter and the other was 1.5mm in diameter, the same diameters as the green and clear fibers respectively). One end of the clear fiber was greased and inserted into the black piece, butted against the green fiber. The clear fiber was either left to coil up on its own, or wrapped around a plastic cylinder roughly

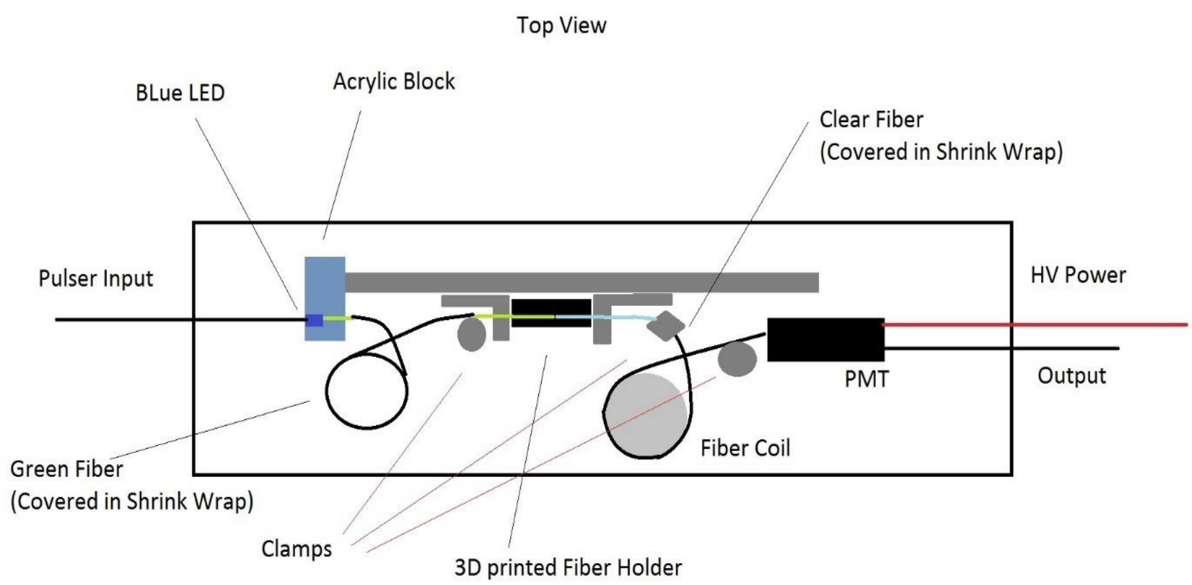

Figure 7: The experimental set-up for testing the transmission length and interface of two fibers.

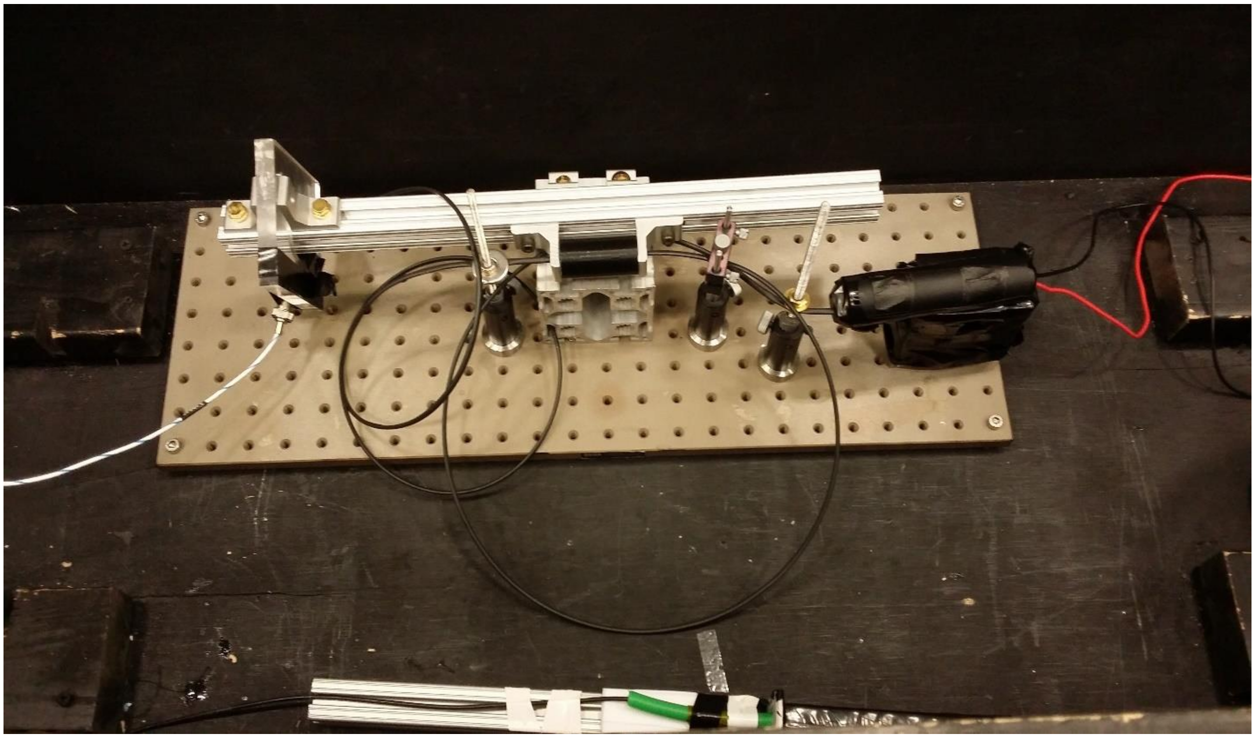

Figure 8: A picture of the same experimental set-up illustrated in Figure 7.

8-10 inches in diameter to hold it, depending on the fiber's length. The other end of the clear fiber was inserted into a black 3D printed block that was taped to the PMT. The fibers were held in place with a series of clamps to keep them from coming loose from their holders.

One final run to test the attenuation length was conducted at a later time that was identical to set up as the previous experiment, described above. There was a key difference in that the 3d printed holder piece was replaced with two stainless steel holders that were screwed together tightly. Each holder had a different size hole in the middle to accommodate the two different fiber diameters. These metal holders were machined to tighter tolerances than the 3d printed piece, allowing them to hold the fibers straight and tight to keep them in line and butted together better than the plastic holder. This was done in the hopes of improving results as the 3d printed piece was somewhat unreliable in holding onto the fibers.

To test the transmission length, a 20-meter clear fiber was inserted, wrapped around the aforementioned cylinder to coil it. The box was closed and the LED and PMT were activated, and signals were recorded. After this, the 20-meter fiber was removed, cut down by 2 meters, the cut end was hand polished and then re-inserted for another run. This was repeated until the meter was 2 meters long, at which point it was cut down to 1 meter. In some cases, where 20 meters of fiber were unavailable, some runs were conducted with shorter lengths of fiber. The average amount of light detected in a light pulse was recorded against the various fiber lengths. This was to ascertain how the light intensity would drop off as the fiber length was increased, as in the final apparatus the fibers will need to be long to reach the SIPMs.

The other point of interest was the fiber interface. Ideally the fibers would be lined up center to center. The fibers are of different diameters, so that does provide some room for one to be slightly off axis without losing light, but it's still very hard to line them up perfectly given their small size. It was to be ascertained how well one must control the fiber to fiber contact to get repeatable results. This was done using a slightly modified set up from the one above. Rather than using a 3d printed fiber holder to hold the fibers perfectly in place, a short (1-2m) clear fiber was held still using clamps while the green fiber's free end was inserted into a clamp that could be moved perpendicular to the axis of the fiber. Two knobs on this clamp allowed one to move the green fiber's end along the 2 axes. For this part, the fiber ends were held centered along each other's axis in the horizontal plane (called 'x' in this case) while the vertical ('y') knob was used to move the fiber ends in and out of alignment in that direction. Each quarter turn of the knob is leads to the clamp translating 0.5mm distance in the given direction. The amount of light detected was measured as a function of the amount the vertical knob was turned. The green fiber was moved all the way to one side such that it was completely out of alignment in the y direction, and the knob was slowly turned while measurements of the light output were taken. This was repeated for three different clear fibers to check repeatability.

Another test for the optical system was a vacuum test of the fiber feed-through. The way this was done was using the set up illustrated in Figure 9. An acrylic window piece was placed in a stainless steel tube connected to a hose leading to a vacuum

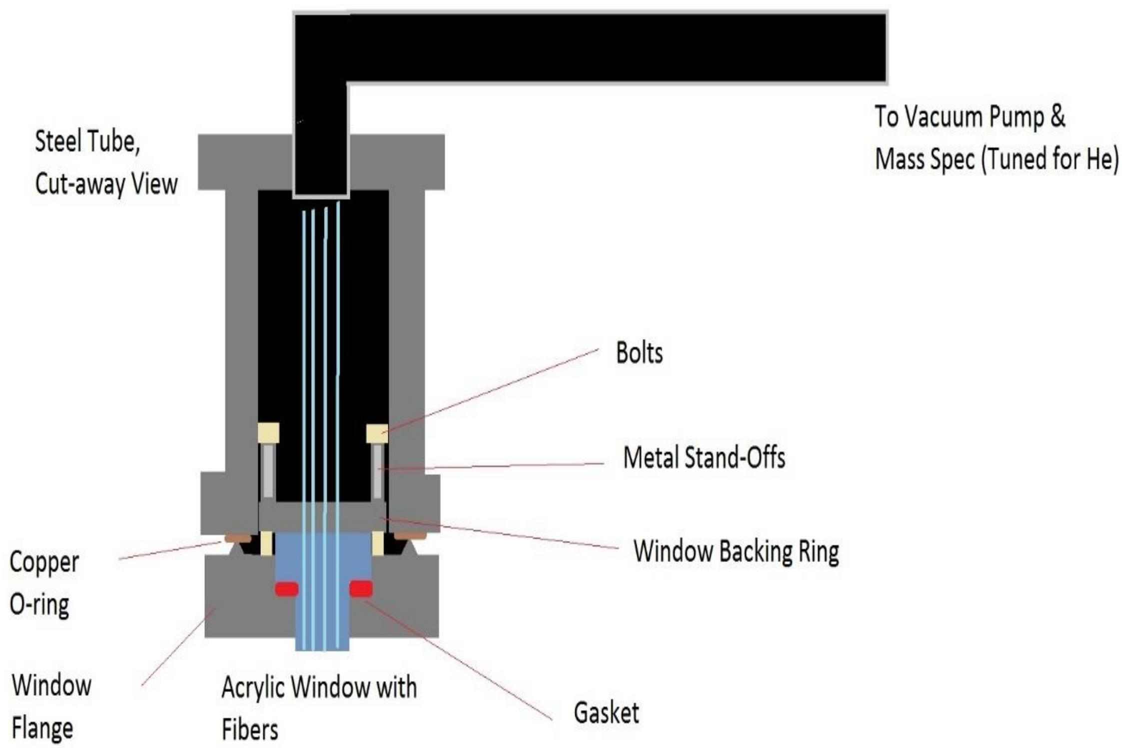

Figure 9: Experimental set-up for testing the vacuum seal on the acrylic window pieces. The window piece is sealed against a flange face by bolting it to the face with a gasket pressed in between them. The backing ring is what is used to bolt the window in place and provides even pressure to the gasket. The vacuum pump pulls any gases present in the tube into a detector which is tuned to look for helium.

pump connected to a Helium leak detector (a mass spectrometer tuned to He). A Teflon gasket was placed between the acrylic window and the window flange. A backing ring was placed on the backside of the acrylic piece and bolted to the flange face to press down on the acrylic piece and the gasket under it. This device was tested to see if Helium gas could leak through it. This was done by taking a Helium tank with a nozzle and spraying a little helium around the window. If any Helium made it into the tube, the vacuum pump would suck it out of the tube, and into a detector which recorded the rate of helium flow into the tube in units of mbar/(liters/second). This unit is analogous to moles per second of helium flowing into the opening. The tests were done at room and cryogenic temperatures. To test this seal in cryogenic conditions, the window was initially submerged into liquid nitrogen in a bucket-like dewar. After some difficulties, the set up was eventually changed to suspend the window just above the surface of some liquid nitrogen, rather than being dunked into it. Some temperature sensors were placed both on the outside and inside of the tube to measure the temperature both on the outer-bottom surface of the tube, as well as inside the tube itself. The helium leak rate was recorded as a function of temperature, during cool down and warm up periods, to ascertain how well the gaskets worked in cold conditions. Initially, a cool-down run was performed before every warm up run, but this practice was stopped after the first five runs. The results for these tests are discussed in the next chapter.

Electronics

As previously mentioned, the electronics consist of four identical SIPMs connected to four identical readout boards. The boards process the signals from the SIPMs and discriminate noise from signal via a threshold voltage setting which was adjusted using a variable resistor. Ideally there is a 'plateau' region where a change in threshold voltage won't change the count rate (which will be true if the smallest signal is well-separated from the noise). The goal was to ascertain where these regions were and how wide they were to figure out where the voltage should be set and how much it could change without affecting results at different temperatures. This was done by placing the boards in a box with a liquid nitrogen feed and temperature controls. The temperature was set to various cold temperatures and the boards were powered on and run. The count rate was measured versus threshold voltage for different temperatures and bias voltages. The next chapter will discuss the results of this and other tests.

CHAPTER FOUR
RESULTS AND DISCUSSION

Measurement Cell

Figure 10 summarizes the light collection runs for the first few runs with a UV LED and the acrylic disk TPB samples in the dark box as well as the runs after overnight room humidity and lab light exposure. Figure 11 shows the light collection as a function of UV exposure time. On Figure 10, the y- axis is the average intensity of the light flashes as given by the average number of photoelectrons initially generated by the PMT, which is proportional to the number of photons incident to the surface of the PMT. The x-axis is just the run number. As one can see, while there are some fluctuations in the graph, the overall pattern is that the amount of light collected remains roughly the same, indicating that taking the samples in and out of the box, as well as leaving them out in the room had no real effect on them. The results also show a large difference in the amount of light that ultimately reached the PMT between the Polypropylene and Polystyrene coatings, with almost double the amount of light reaching the detector through a sample coated in a polypropylene and TPB film (53% light transmission as compared to an empty run) as compared to polystyrene (32% as compared to an empty run). The results also show that with no coating, very little light would reach the PMT due to it being blocked out by the PMMA as indicated by the results of the empty and blank runs. However, it also shows that a significant amount of light is lost at the TPB coating, as seen by the empty run, since and empty run produces about twice as much light as when a Polypropylene TPB coating is used.

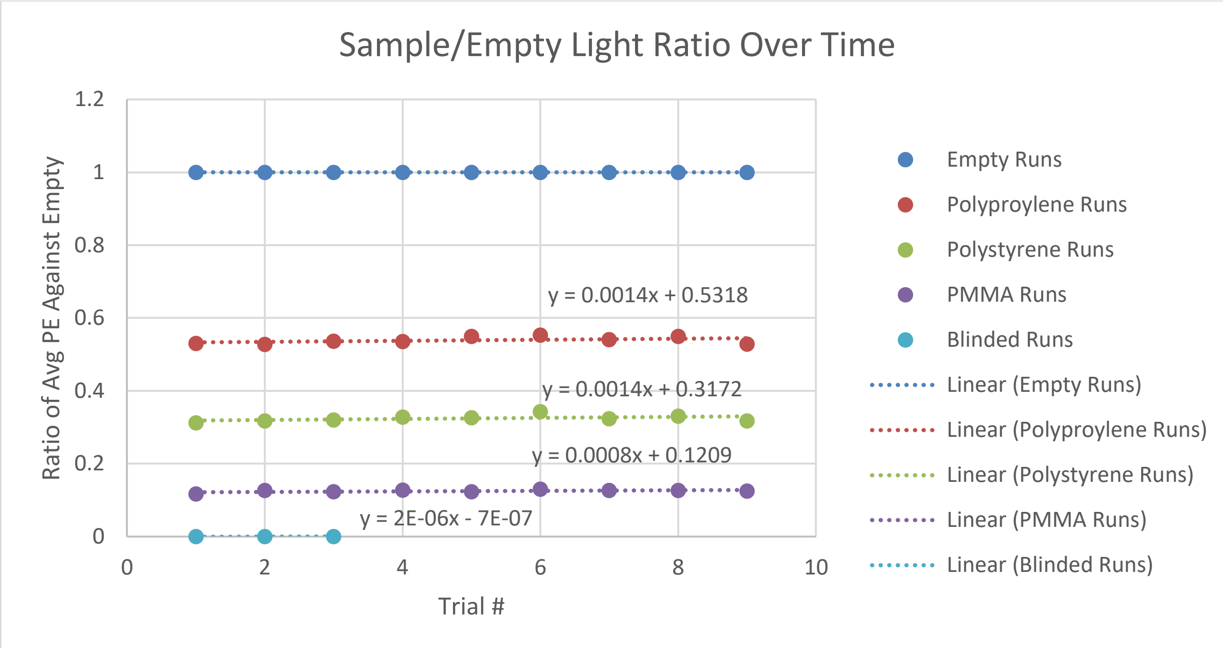

Figure 10: Results of the light transmission runs not including those involving UV exposure.

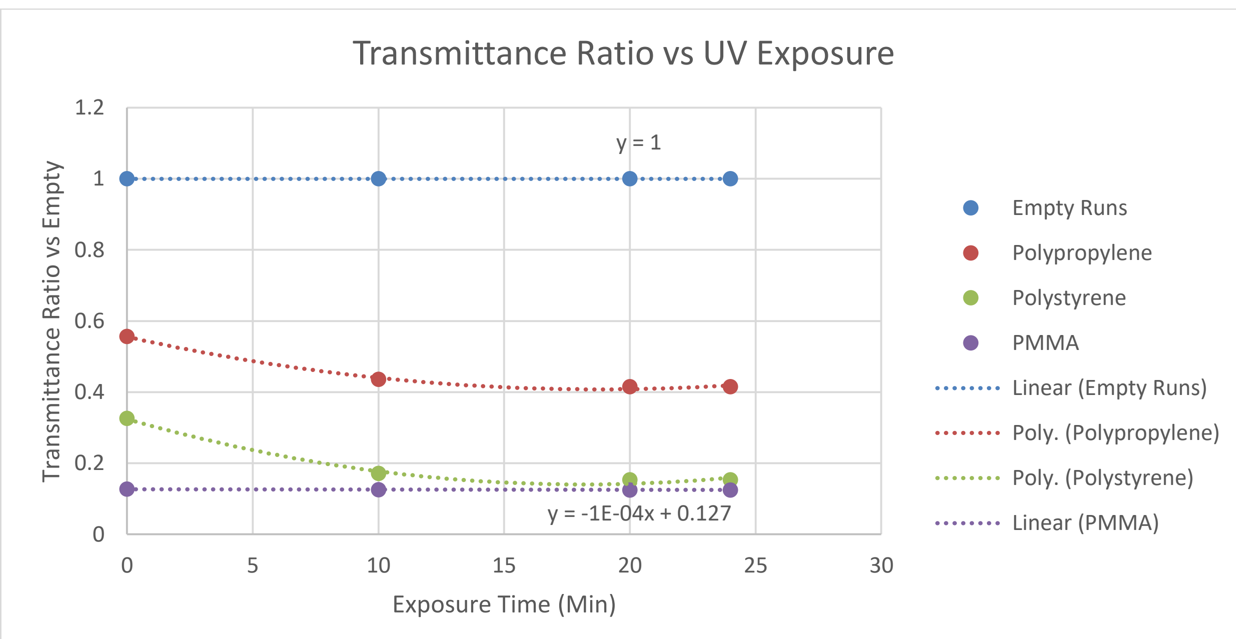

Figure 11: Results of the light transmission runs after the samples were subjected to increasing times of sunlight exposure.

UV exposure was a different matter. After about 24 minutes of exposure, a noticeable decrease in the amount of light detected by the PMT was seen, as illustrated in Figure 11. After about 24 minutes of exposure, the amount of light detected through a Polypropylene TPB coating dropped to around 75% its initial level. The Polystyrene TPB coating saw its light transmission levels from to 50% its initial level until it was no better than a blank PMMA disk. Acrylic (PMMA) is a poor transmitter of UV light, as seen by the PMMA baseline produced by the blank disks. If the TPB samples are losing their ability to transmit UV light, it seems likely that what's happening is that the TPB becomes less able to convert the UV light from the LED to visible light, and in turn the PMMA disks backing the TPB are then blocking the UV light from reaching the PMT. For the second set of TPB sample runs, the same general pattern is seen in that the amount of light detected does not fall with lab light exposure, but UV exposure will cause decay. However, the numbers are somewhat different as seen in Figures 12 and 13. For example, the amount of light let through with a Polypropylene sample in the second run was roughly 30% that of an empty run. In the first set of runs it was roughly 50%. Likewise, the other numbers are also low. It's hard to say why these percentages are different. The coatings on the sample disks and TPB wafer were not uniform, being more transparent in some places than others. The orientation of the sample disks may affect results as it may make the LED face areas with thicker or thinner coatings. It's also possible that the coatings were not uniform between the 2 different sets.

Sun exposure is a bit of an extreme as the UV scintillation light isn't nearly as intense or as long lived as 10 minutes of sun exposure, it does show that the TPB can

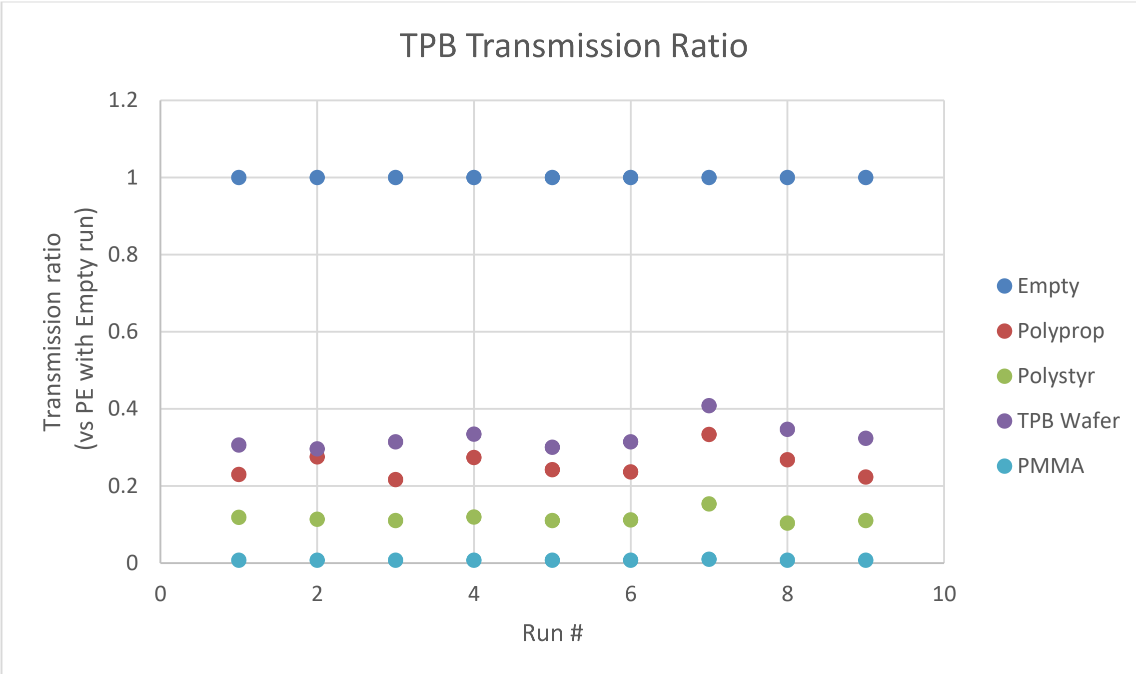

Figure 12: The results of the second set of TPB sample checks.

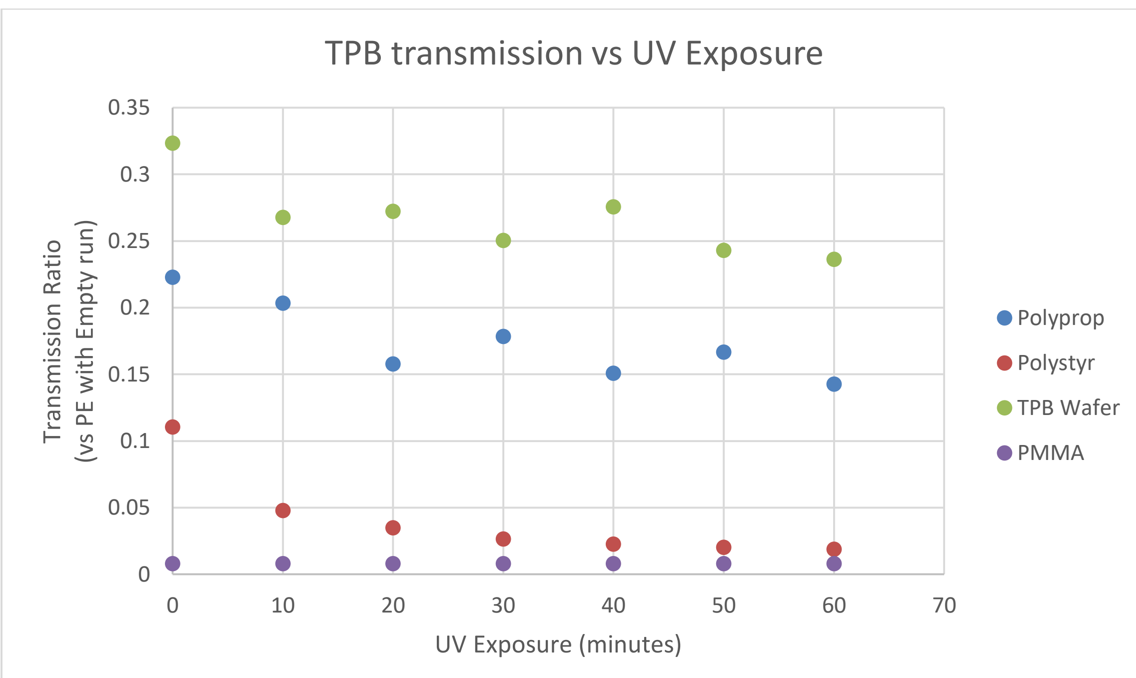

Figure 13: The results of the second set of TPB sample runs with an hour of total UV exposure.

‘wear out’ so to speak. If repeated measurements are taken for long periods of time with the same coating of TPB on the measurement cell, one may expect a small decrease in the amount of light being transmitted to the optical transport system, but not enough to emulate sun exposure. For reference, roughly 1000W/m^2 of solar light is incident on Earth’s surface, of which less than 5% is UV light around 250-300nm [11]. The TPB disks are approximately 2.5cm in radius, so in 10 minutes’ time the disks saw approximately 60J of energy. If one assumes the UV photons striking it were around 280nm in wavelength, then approximately 8.5x10^19 photons struck the each of the disks in 10 minutes. For comparison, the measurement cells will see about 10^11 photons/cm^2. A patch of the cell of the same size as the disks would see many orders of magnitude fewer photons than the disks saw from the sun. This means one should not expect too drastic a decrease in the transmittance of the TPB coatings due to scintillation light exposure, especially if the TPB coating is applied with Polypropylene.

Optical System

The results from the transmission length check were inconsistent, as seen in Figures 14 & 15. The transmission length from the graphs is seen to be anywhere from 5 to 37 meters. This was hypothesized to be due to the experimental set up. Due to the nature of 3D printing, object sizes can vary, particularly when holes are involved. In the 3D printing process, a plastic filament (In this case ABS) is heated to its glass transition temperature and is laid down in layers to form a solid object. As the object cools during and after printing, some warping can occur. This can cause the dimensions of the object to be slightly off. When printing an object with holes, one

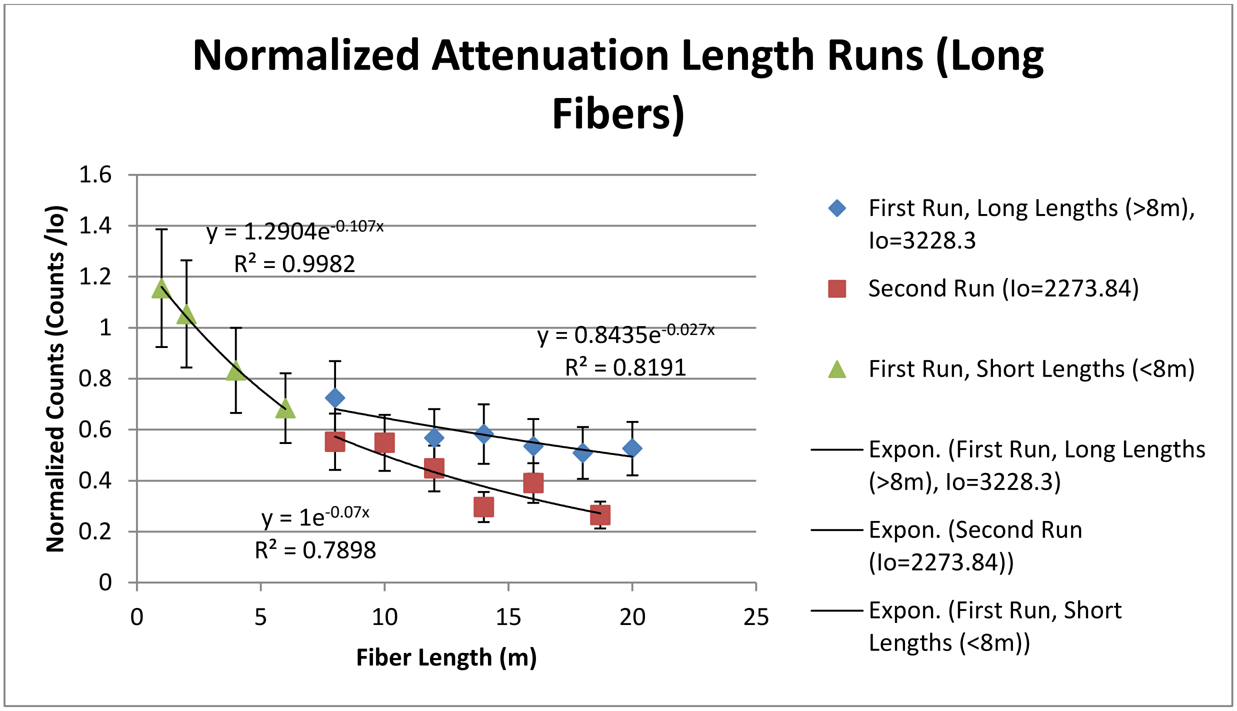

Figure 14: The first two attenuation length runs. The first run is separated in two parts, short fiber lengths (blue points) and long fiber lengths (green points).

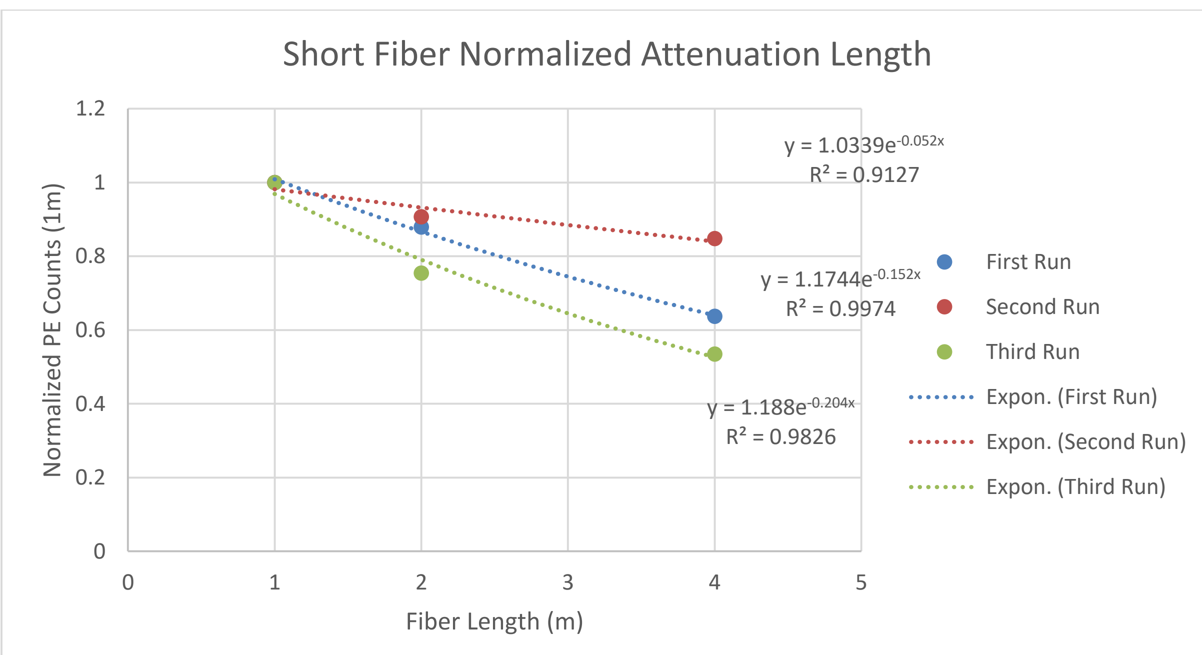

Figure 15: The results of the three short fiber runs.

generally must oversize them in the object file before printing as they will turn out smaller in real life. This was attempted with the black holder piece, but was done with very limited precision, so the piece had a loose fit for the fibers. It's possible they were able to move out of alignment with each other or away from each other enough to cause some light losses between different runs, throwing off precision.

Other possible contributions to the lack of precision in and between the runs may have to do with the fact that the ends of the clear fiber were polished by hand every time it was cut down. There may have been inconsistencies in the way it was cut and polished. For example, a cut may have been slightly angled, leading to the fibers not sitting flush. Also, during polishing some of the outer cladding could've come off and got stuck to the end of the fiber, obstructing the light coming through. To test this, multiple fibers that were all 2 meters long that were hand-polished were individually tested to see the difference in the amount of light collected. In the end there was about a 15-20% difference in measured light between multiple fibers of similar preparation, as seen in Figure 16.

It was also to be ascertained how much measurements could vary between runs with the same fiber, as can be seen in Figure 17.   To quantify this, a 1-meter fiber was plugged into the apparatus. A light measurement would be taken, then the power supply turned off, the fiber removed and re-inserted, and the whole process repeated. This was meant to simulate swapping out fibers between each run of the attenuation length experiment. This was conducted at regular intervals over two hours to see what impact it would have on the amount of detected light. While the PMT was left to run for

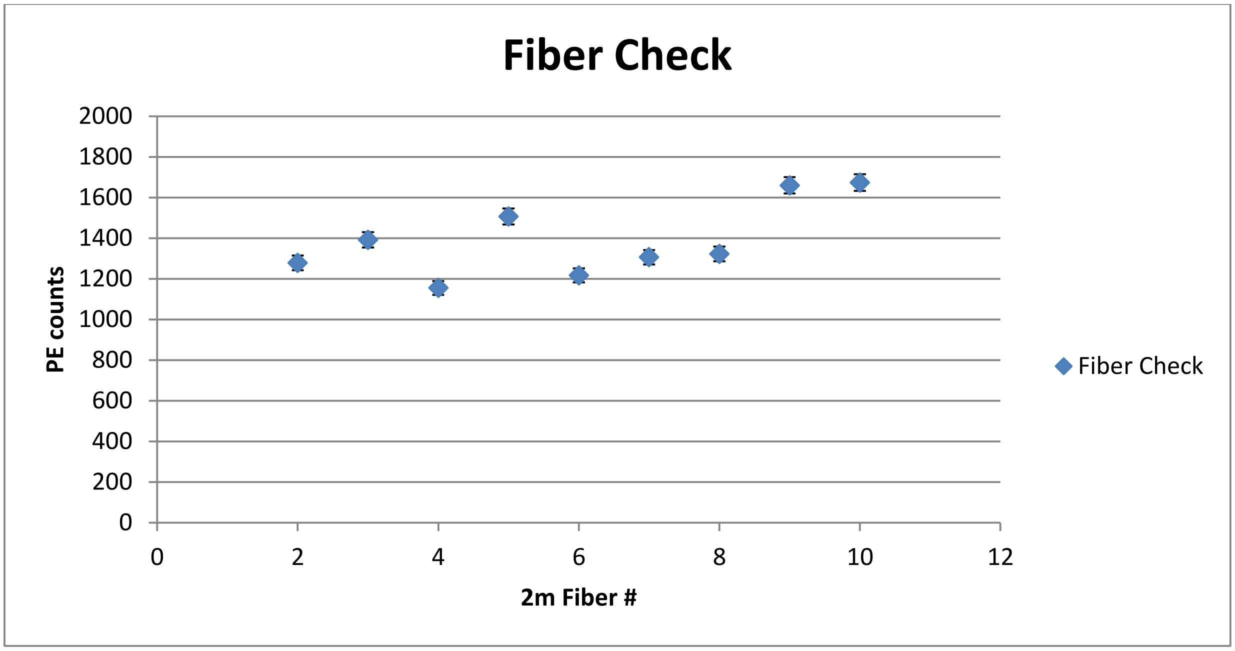

Figure 16: The results of the 2m Fiber check. Different 2 meter fibers were hand prepared, then measured for the amount of light transmitted. There's about 15-20% variation between fibers.

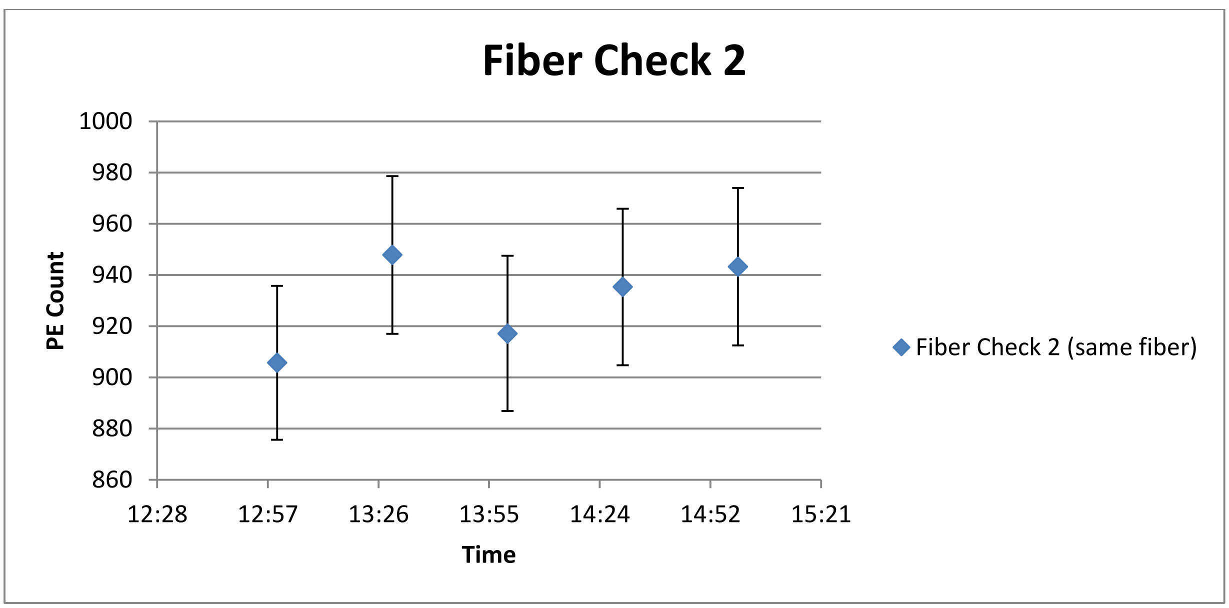

Figure 17: The results of leaving the PMT running for the majority of 2 hours with the same fiber. There's only a 5% variation between the different runs.

2 hours, a slight increase could be seen in the counts. There was only a small variation of about 5% between the runs, and the points are within statistical error for each other, so there is not much variation seen with the same fiber.

It's worth noting that shorter wavelengths of light will attenuate faster than longer wavelengths in the fibers as they are more readily absorbed. If one looks at a graph of the Intensity of light over different fiber lengths, they will find the attenuation coefficient changes between short and long fibers [9]. However, this effect should be minimized since the light was passed through a wavelength shifting fiber that should've narrowed the spectrum of light seen to visible wavelengths around green. Even so, in Figure 14 one can still see a noticeable change in the behavior of the graph between short (<8m) and long (>8m) fibers.

Some of this may be due to different mechanics by which light can be trapped in the fiber which may produce different attenuation coefficients such as meridional and skew trapping or via trapping light in the cladding of the fiber [13].

The results of the last attenuation length experiment can be seen in figure 18. With this last run, an attenuation length of 27 meters was observed. The results for this last run have a more precise fit to an exponential decay trend line than previous runs. Since the major difference in this run was the machined fiber holder, it stands to reason that the tighter fit provided allowed for more consistent results.

The graphs from the fiber alignment experiments are shown in Figure 19. With the green fiber starting at the top-most position at 0 turns with the y-axis knob, and 8 being the maximum number of turns, the 2 fibers were aligned center to center at 4

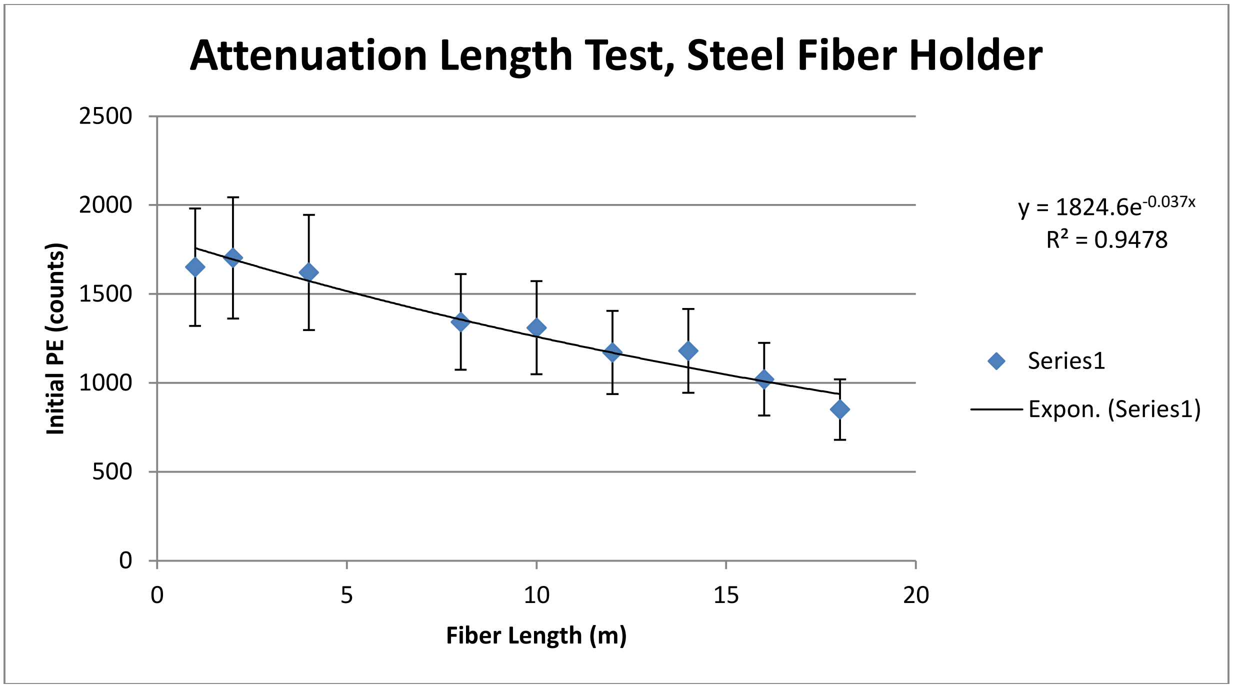

Figure 18: The results of the final Attenuation length run with a machined fiber holder.

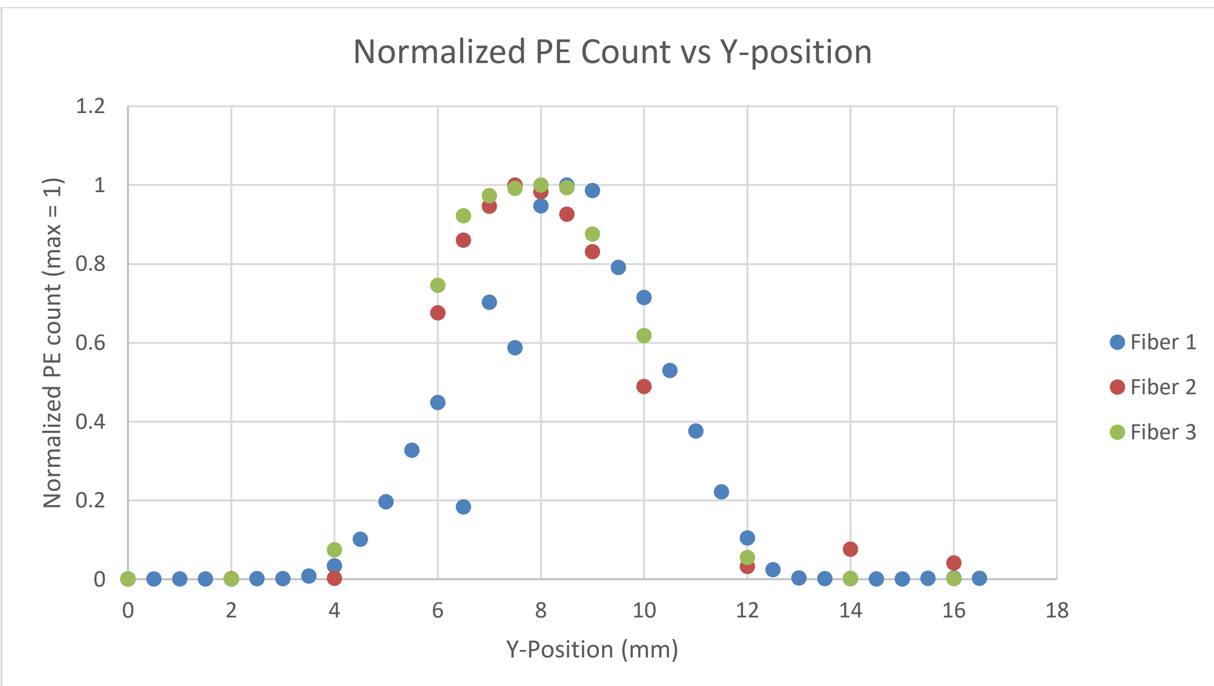

Figure 19: The results of the 3 fiber interface checks.

turns. To translate this into units of length, 8.5 turns on one of the knobs produces roughly 4.25mm of translation for a ratio of 0.5mm per turn. As one might expect, each of the three graphs shows maximum light intensity at around 4 turns of the y-knob. It was expected that the amount of light detected would plateau near the center for 2 or 3 quarter-turns due to the fact that the green fiber is 0.5mm smaller in diameter, meaning all of the light leaving it can still be captured by the other fiber over a small amount of misalignment. Outside of that, the detected light levels drop off quickly, which would indicate that in the final experiment, taking care to align the fibers within a 0.5mm difference axis to axis will be important to avoid losses. However, it is worth noting that the absolute number of photoelectrons varied from fiber to fiber. The green fiber was never replaced with another, and the 3 clear fibers were of the same length and were prepared the same way with regards to how they were cut and polished, so it seems that they should yield the same results. It would seem most likely that the differences can be contributed to sample preparation, as the fibers were both polished and butted together by hand.

The compiled vacuum seal results can be seen in Figures 20 & 21. The first graph shows the leak rate against the temperature as the setup was warming up after having already been chilled. The second shows the leak rate during the cool-down itself. Multiple setups were tried. Originally, steel bolts were utilized to tighten the backing ring with no bolt standoffs and a metal backing ring. Eventually the 8 steel bolts were switched out for twice as many bolts made of PEEK polymer. The polymer bolts contract at a higher rate than steel, allowing them to keep more tension on the gasket.

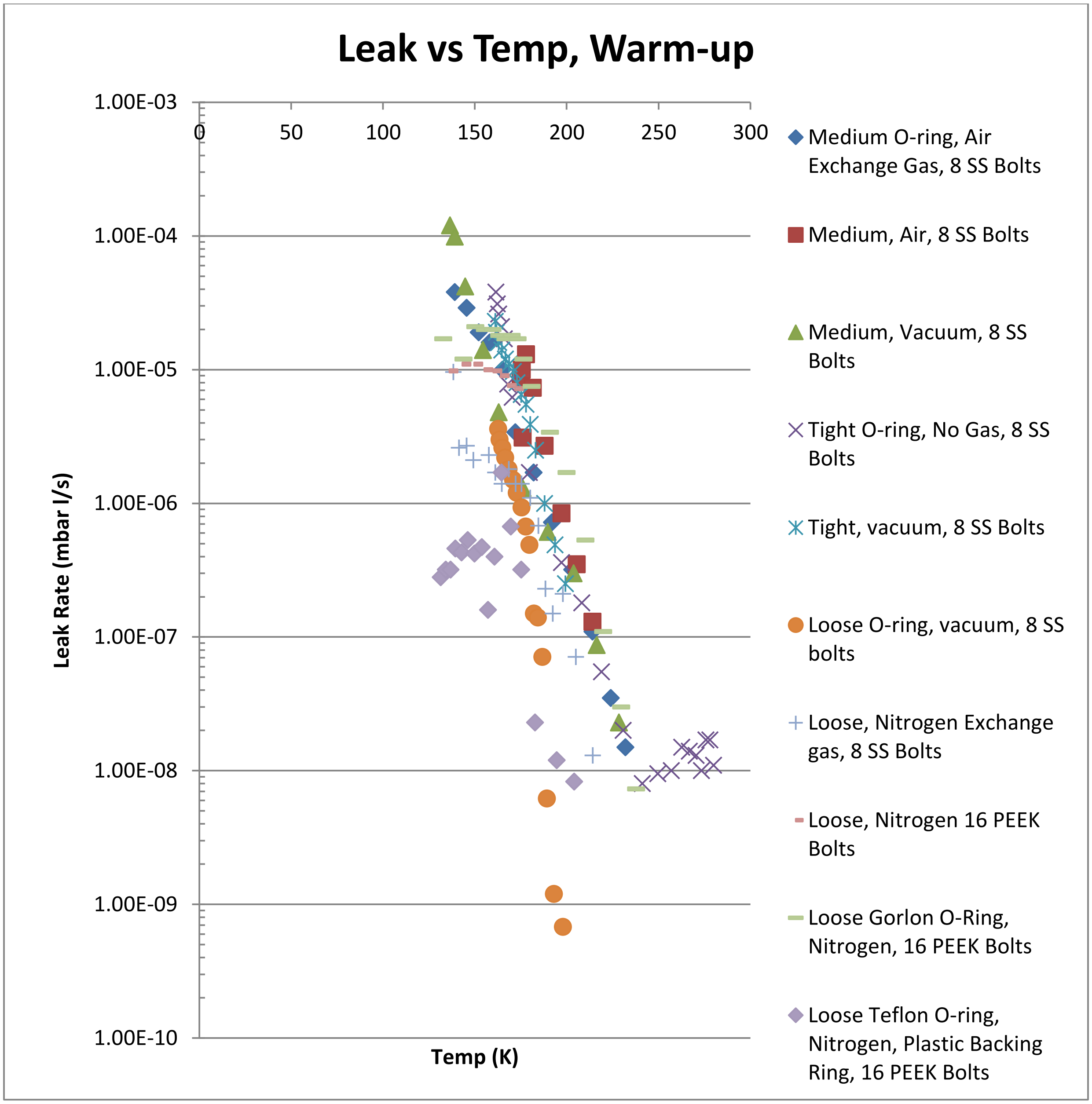

Figure 20: A compiled view of the various leak checks as the temperature rose as the tube was warmed up.

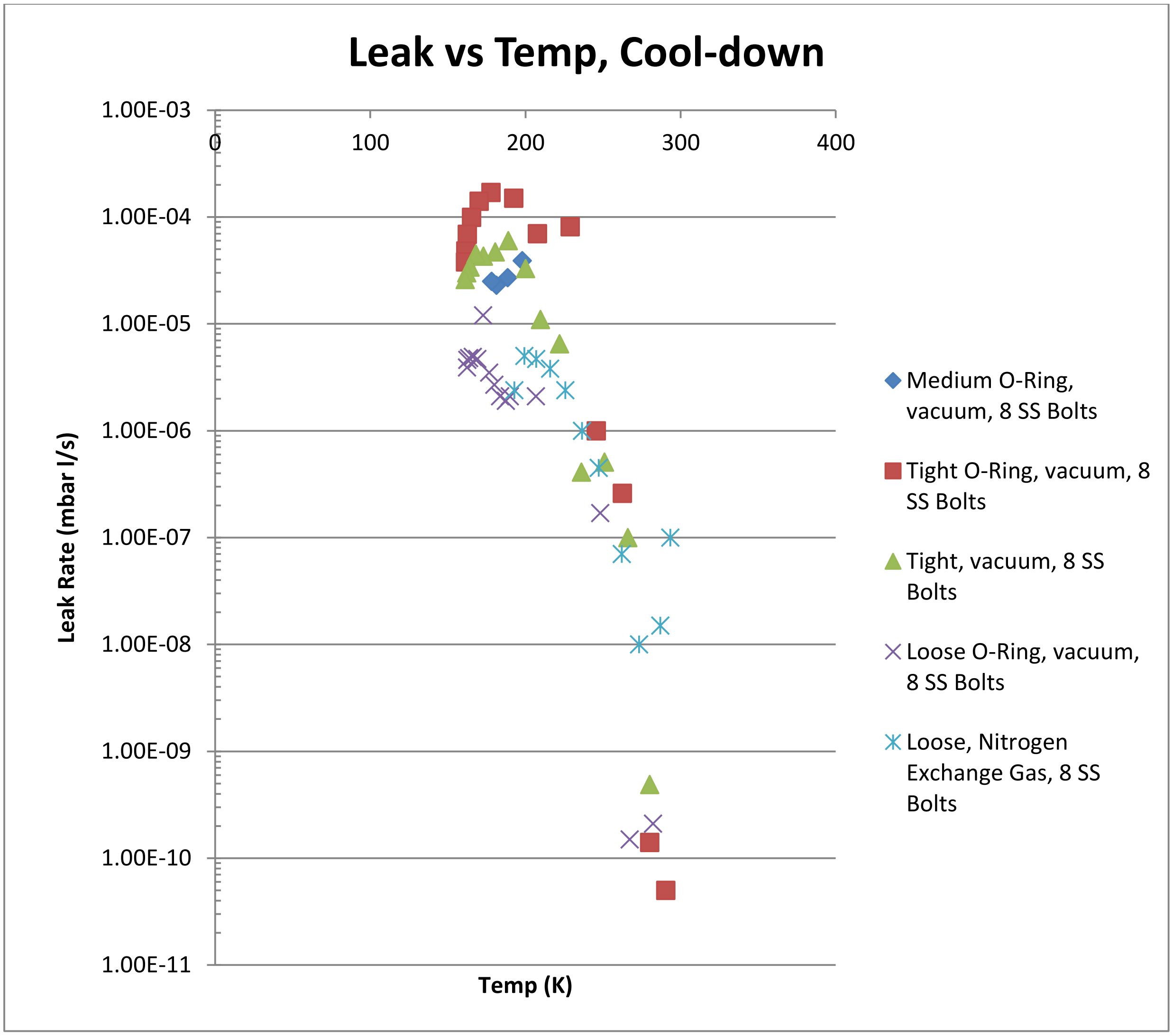

Figure 21: A compiled view of the leak checks done on the tube as it was being chilled.

However, it still wasn't enough, so metal standoffs were later slipped on over the PEEK bolts. When the PEEK bolts and acrylic shrank, the standoffs did so at a slower rate, offsetting the difference enough to lower the leak rate. Different gasket ring sizes were utilized as well, with an average sized ring being used for the first few runs, then a small, tight gasket was utilized, and finally a large, loose fitting ring was used. It was found that larger rings provide a slightly better seal whilst tight ones run the risk of introducing stress to the acrylic and causing it to crack. The very last warm-up run was the best in terms of having a low, stable leak rate at low temperatures. This run was achieved with a polymer backing ring, PEEK bolts, and metal standoffs. This combination seems to maintain tension on the gasket at low temperatures better than the others.

Electronics

Figure 22 shows the results of the threshold runs. At lower temperatures, the rise in count rate at low thresholds is very similar. In that regard, setting the threshold low will yield very similar results at lower temperatures. At higher thresholds, the point at which the count rate begins to drop off varies more between temperatures. If this should be problematic, it would seem that setting the boards to a low threshold should help. In general, the colder the boards get, the narrower the plateaus become. The final experiment will be able to control Threshold voltages down to 1mv increments, temperature at 10K increments, and Bias voltage at 0.1V increments. The plateau values between different low temperature runs show that the Threshold voltage window is around 5 or 6 mV, which is bigger than the control increments. One can see that

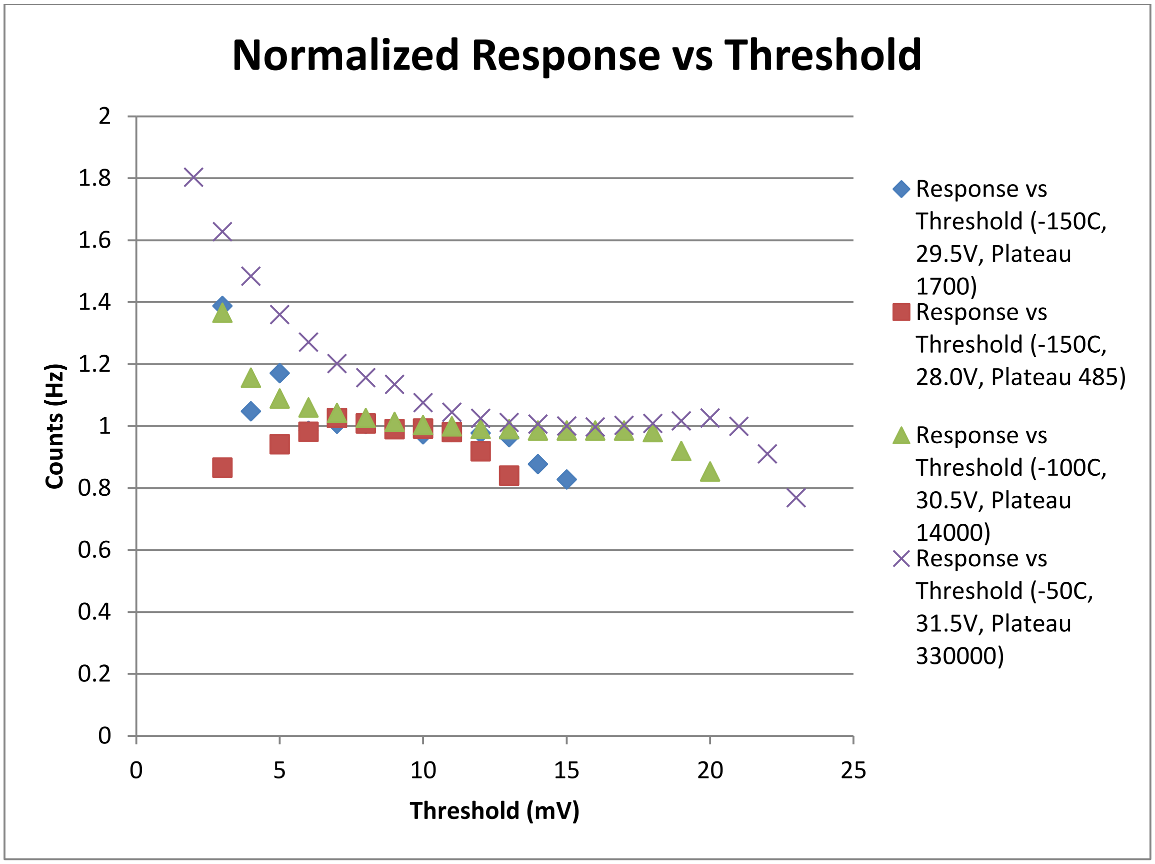

Figure 22: The Compiled Results of the threshold checks at different temperatures. Vbias increases approximately 1 volt for every 50 degrees Celsius the temperature drops to maintain overvoltage.

between -150 and -100 Celsius, the threshold window still stays plenty wide. With changes of up to 1.5 volts it also stays wide. Given how fine the controls on the experiment are, this gives plenty of room to work with, so small fluctuations shouldn't be catastrophic for the final experimental results.

CHAPTER FIVE
CONCLUSION

In conclusion, the keys to securing accurate measurements in the coming nEDM experiment will revolve around a few things: maintaining the seal (to prevent helium from reaching the upper compartment, ruining the vacuum, and acting as an exchange gas that will let the upper compartment heat up), ensuring good optical interfaces (by properly aligning optical fibers nearly center to center), knowing how to minimize light losses (knowing how light attenuates with different fiber lengths, choosing optimal TPB coatings, and knowing how the TPB coating may decrease in efficiency with exposure to UV light), and choosing voltage settings that ensure stable readings (e.g., setting bias and threshold voltages such that changes in temperature won't cause large increases or decreases in the amount of signals). Maintaining temperatures and setting robust thresholds should prevent drastic changes in the count rates of the boards or drops in efficiency, which is important because they are being used to try to accurately measure light from the cell to ascertain an event rate over time. Maintaining good fiber alignment will minimize the amount of light lose between two fibers at their interface, allowing more to be eventually detected, improving the statistics of the measurements. Knowing how light will attenuate in long fibers and how much TPB's light transmission changes over time will allow one to properly design and set up the experiment.

WORKS CITED

[1] Fillipone, Brad. *Neutron Electric Dipole Moment.* NIST Center for Neutron Research Summer School June 2009.
http://www.ncnr.nist.gov/summerschool/ss09/pdf/Filippone_FP09.pdf

[2] Chapter 2: Baryons, Cosmology, Dark Matter and Energy. Institute for Nuclear Theory, University of Washington.
http://www.int.washington.edu/PHYS554/2011/chapter2_11.pdf

[3] Griffiths, David. Introduction to Electrodynamics, 4th Ed. Pearson, 2013. Pg 172.

[4] Joram, C. *Transmission Curves of Plexiglass (PMMA) and Optical Grease*. 2009. CERN Document Server. http://cds.cern.ch/record/1214725/files/PH-EP-Tech-Note-2009-003.pdf

[5] Jerry, R. Winslow, L. Bugel, L. Conrad J.M. *A Study of the Fluorescence Response of Tetraphenyl-butadiene.* Physics.ins-det article 1001.4214v1

[6] Franchi, R. Montereali, R.M. Nichelatti, E. Vicenti, M.A. Canci, N. Segreto, E. Cavanna, F. Di Pompeo, F. Carbonara, F. Fiorillo, G. Perfetto, F. *VUV-Vis Optical Characterization of Tetra-phenyl-butadiene Films on Glass and Specular Reflector Substrates from Room to Liquid Argon Temperature.* Physics.ins-det article 1304.6117

[7] Linear Expansion. http://hyperphysics.phy-astr.gsu.edu/hbase/thermo/thexp.html

[8] The Engineering Toolbox. *Coefficients of Linear Thermal Expansion.*
http://www.engineeringtoolbox.com/linear-expansion-coefficients-d_95.html

[9] Knoll, Glenn F. *Radiation Detection and Measurement, 4th Ed.* John Wiley & Sons, 2010.

[10] Introduction to the SPM, Technical Note. Sensl, 2011. www.sensl.com

[11] Baghzouz, Y. *Sunlight and its Properties.* University of Nevada, Las Vegas, College of Engineering. http://www.egr.unlv.edu/~eebag/Sunlight%20and%20its%20Properties.pdf

[12] *Hyperphysics: Beats.* Georgia State University department of Physics and Astronomy. http://hyperphysics.phy-astr.gsu.edu/hbase/sound/beat.html

[13] Arkin, William T. *Focus on Lasers and Electro-opics Research.* Nova Science Publishers, New York. 2004.

VITA

Patrick Rogers was born in Richmond, Kentucky. He enjoyed studying mathematics and physics in high school and in undergraduate university. He became a physics major in his third year at Eastern Kentucky University and graduated with a Bachelor's Degree in general physics and minors in chemistry and mathematics. He went on to the University of Tennessee in Knoxville to pursue a Master's in physics and graduated in May 2017.